ISSN 0005–1144
ATKAAF 46(1–2), 83–91 (2005)

Domenico Casadei, Giovanni Serra, Angelo Tani, Luca Zarri

Experimental Behavior of a Matrix Converter Prototype Based on New Power Modules

UDK 621.316.543
IFAC 5.5.4

Original scientific paper

This paper describes the design and the solutions adopted for a matrix converter prototype of 10 kW, based on new integrated power modules. The performance of the converter is verified by means of experimental tests.

Key words: matrix converter, converter drive system, modulation strategy, current commutation strategy, integrated electronic power module

1 INTRODUCTION

A matrix converter (MC) is an array of controlled semiconductor switches that directly connect each input phase to each output phase, without any intermediate dc link. The main advantages of the MC are the absence of bulky reactive elements, that are subject to ageing and reduce the system reliability. Furthermore, MC provides bidirectional power flow, nearly sinusoidal input and output waveforms and a controllable input power factor. Therefore MCs have received considerable attention as a good alternative to voltage-source inverter (VSI) topology.

The development of matrix converter prototypes started when Alesina and Venturini proposed the basic principles of operation in the early 1980's [1]. Afterwards the research in this fields continued in two directions. On the one hand there was the need of reliable bidirectional switches, on the other hand the initial modulation strategy was abandoned in favor of more modern solutions, allowing higher voltage transfer ratio and better current quality.

As regards the modulation strategies, in the original theory the voltage transfer ratio was limited to 0.5, but it was shown later that, by means of third harmonic injection techniques, the maximum voltage transfer ratio could be increased up to 0.866, a value which represents an intrinsic limitation of three-phase matrix converters with balanced supply voltages [2]. A new intuitive approach towards the control of matrix converters was presented in [3]. As known, this approach is also defined »indirect method«, because the matrix converter is described as a virtual two stage system, namely a 3-phase rectifier and a 3-phase inverter connected together through a fictitious DC-link. The indirect approach has mainly the merit of applying the well-established space vector modulation (SVM) for VSI to MCs, although initially proposed only for the control of the output voltage [4]. The SVM was successively developed in order to achieve the full control of the input power factor, to fully utilize the input voltages and to improve the modulation performance [5, 6]. A comparison between different types of modulation strategies can be found in [7, 8], showing that the »indirect approach« for MCs, initially preferred for its simplicity, is now partially replaced by modern direct theories, that allow an immediate understanding of the modulation process, without the need of a fictitious DC link.

In the meantime several studies were presented about the bidirectional switches necessary for the construction of a MC. The bidirectional switches were initially obtained combining discrete components [9]. Then, as the interest toward MCs increased, some manufacturers produced power modules specifically designed for MC applications [10]. As regards the hardware components, the switches are usually traditional silicon IGBTs, but also other solutions have been recently tested, such as MCTs or IGBTs with SiC diodes. The performance of the switches has been compared in [11–13].

Another problem that the researchers have overcome is the current commutation between the bidirectional switches. The absence of free-wheeling diodes obliges the designer to control the commutation in order to avoid short circuits and over voltages. A comparison among several solutions has been done in [14] and [15].

To obtain a good performance of the MC, it is necessary also the design of a L-C filter to smooth the input currents and to satisfy the EMI requirements [16]. It has been shown that the presence of a resonant L-C filter could determine instability phenomena that can prevent the MC to deliver the rated power to the load [17]. A possible remedy for this problem consists in filtering the input voltage before calculating the duty-cycles. In this way it is possible to increase the stability power limit and to obtain the maximum voltage transfer ratio.

Some prototypes of MC have been already designed [18–20]. In this paper the construction of a 10 kW matrix converter using new IGBT modules is described. All the solutions adopted to achieve a good performance are presented and practical results are given.

2 STRUCTURE OF MATRIX CONVERTERS

Basically, a MC is composed by 9 bidirectional switches, as shown in Figure 1.

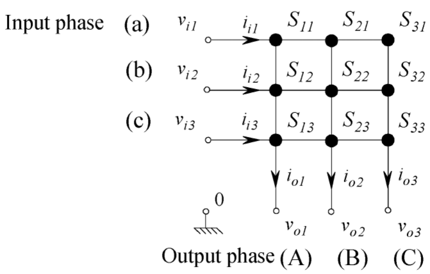

Fig. 1 Basic scheme of matrix converters

The converter is usually fed at the input side by a voltage source and it is connected to an inductive load at the output side. The schematic circuit of a MC feeding a passive load is shown in Figure 2. The system is composed by a voltage supply, an L--C input filter, the MC and a load impedance.

The input filter is generally needed to smooth the input currents and to satisfy the EMI requirements. A reactive current flows through the input filter capacitor, which results in a reduced power factor especially at low output power. As a consequence, the capacitor is chosen in order to assure at least a power factor of 0.8 with 10 % of the rated output power. After the selection of the capacitor, the input filter inductance of the MC can be chosen in order to satisfy the IEEE Recommended Practices and Requirements for Harmonic Control in Electrical Power Systems (IEEE Std. 519-1992). If the input filter is well designed, current harmonics at frequencies greater or equal to the switching frequency are adequately smoothed.

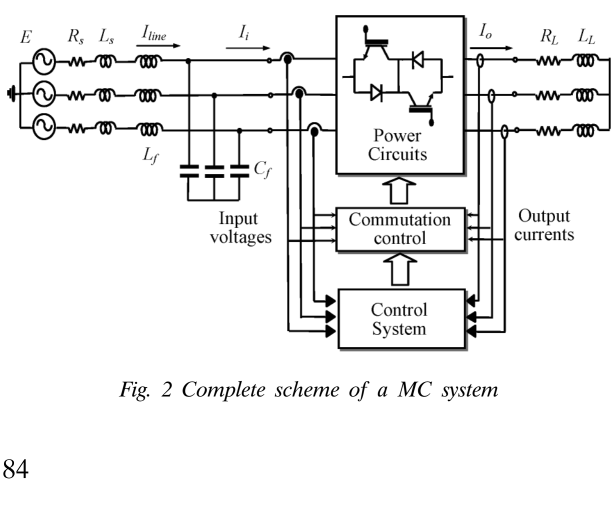

Fig. 2 Complete scheme of a MC system

3 INPUT CURRENT MODULATION STRATEGIES

As known, the MC allows the control not only of the output voltages, but also of the phase angle of the input current vector.

There are several possible solutions for the modulation of the input current vector that basically differ in the direction along which the current vector is modulated. This direction can be represented introducing an arbitrary vector $\overline{\psi}$, here named »modulation vector«. A modulation strategy is completely defined once the modulation vector $\overline{\psi}$ is assigned.

For any strategy it results

$$\psi \cdot j\,\overline{i_i} = 0 \tag{1}$$

where $\overline{i_i}$ is the input current vector. If the switches are assumed ideal and the converter power losses are neglected, the input current vector can be expressed as follows:

$$\overline{i_i} = \frac{2}{3}\frac{p_o}{\overline{v_i} \cdot \ \overline{\psi}}\overline{\psi} \tag{2}$$

where p_o is the power delivered to the load.

The input current space vector depends on the output power level, the input voltage vector and the modulation vector. Once the modulation vector is chosen, this expression can be further developed. Theoretical and experimental results obtained comparing some input current modulation strategies are given in [21] and [22].

A. *The input current vector is kept in phase with the input voltage vector (Strategy A)*

The simplest input current modulation strategy is to keep the input current vector in phase with the actual input voltage vector, determining instantaneous unity input power factor, as follows:

$$\overline{\psi} = \overline{v}_i . \tag{3}$$

It is worth noting that in case of input voltage distortion, input currents cannot be sinusoidal. It could be shown that the k^{th} harmonic in the input voltage leads to input current harmonic of order k^{th} and $(2\text{-}k)^{th}$.

B. The input current vector is kept in phase with the fundamental component of the input voltage vector (Strategy B)

In [21] it was demonstrated that a better performance in terms of input current distortion can be achieved if the input current vector is kept in phase with the positive sequence fundamental component of the input voltage vector.

In order to obtain the positive sequence fundamental component, the input voltage vector can be filtered by means of a digital filter. Hence, the input current vector is kept in phase with the filtered input voltage vector $\overline{v}_{if}$. Therefore, the modulation vector $\overline{\psi}$ is defined by

$$\overline{\psi} = \overline{v}_{if}. \tag{4}$$

It is possible to demonstrate that this strategy represents the optimal modulation strategy which determines the lowest total RMS value of the input current disturbance. It will be pointed out that this strategy also has a stabilizing effect on the converter operation.

For these reasons, Strategy B has been adopted for the MC prototype described in this paper.

4 INSTABILITY PHENOMENA

The simplest voltage modulation strategy is based on detecting the zero crossing of one input voltage for synchronizing the input current modulation. This control technique performs correctly assuming an ideal power supply (i.e. balanced and sinusoidal supply voltages), but in presence of input voltage disturbances, these are reflected on the output side determining low-order voltage harmonics, as the MC has no internal energy storage. Considering unbalanced non-sinusoidal input voltages, the magnitude and the angular velocity of the input voltage vector are not constant. Then, a simple synchronization with the input voltages is no longer applicable but the input voltages must be measured at each cycle period, in order to calculate the duty-cycles necessary to generate balanced and sinusoidal output voltages.

However, the compensation of the input voltage disturbances achieved by this control strategy might lead to instability phenomena when the MC output power exceeds a maximum limit. The waveforms of

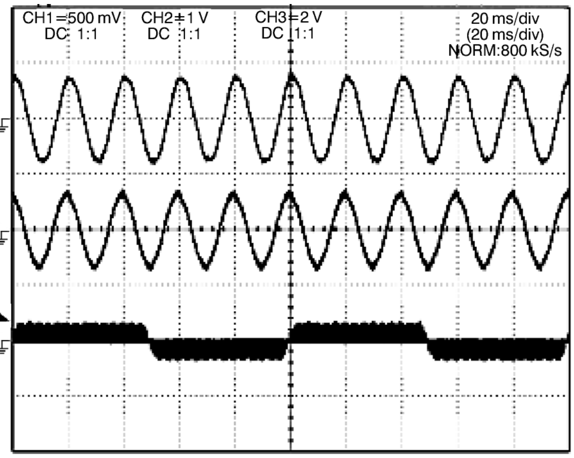

Fig. 3 Experimental tests: stable steady state operation. Upper track: line current (20 A/div). Middle track: input line-to-neutral voltage (400 V/div). Lower track: load line-to-line voltage (600 V/div)

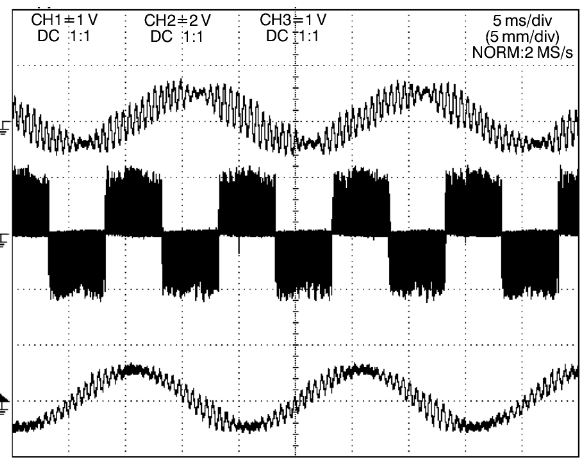

Fig. 4 Experimental test: unstable steady state operation. Upper track: line current (10 A/div). Middle track: line to line output voltage (400 V/div). Lower track: line to line input voltage (400 V/div)

the line current, the output voltage and the input line-to-line voltage during stable and unstable operation are shown in Figures 3 and 4 for a 10-kW MC.

Here is a qualitative explanation of the instability phenomena. Let's suppose that a voltage disturbance is temporarily applied at the converter input, thus leading to a variation of the input current. It is worth noting that this current variation is proportional to the output power. The current harmonics with frequencies near the resonant frequency of the LC input filter are amplified and their effect is to reinforce the input voltage disturbance. If the output power is small, this reinforcement action is too weak and after the disturbance has vanished, the converter returns to the normal steady state operation. Otherwise, if the output power is high enough, the reinforcement action is sufficient to establish self-sustained oscillations in the input voltages, even when the initial disturbance has vanished. In this case, the system reaches a new steady state operation, but the converter does not work correctly because the input currents and voltages are severely distorted. It is interesting to note that these oscillations have the form of »beatings«, namely they are composed by at least two separate harmonics with close frequencies.

A first attempt to determine the stability power limit was done in [23], where the stability is evaluated by analyzing the migration of the eigenvalues of a small-signal model of the system. The power limit results as follows:

$$P_{lim} = \frac{3}{2} V_i^2 C_f \sqrt{\frac{R_s^2}{L_T^2} + 4\omega_i^2} \tag{5}$$

where V_i is the amplitude of the input voltage vector, ω_i the input angular frequency, and L_T is the sum between filter and line inductances. For a prefixed value of the input filter resonance frequency, (5) emphasizes that, in order to increase the power limit, high values of the capacitance C_f and low values of the inductance L_f should be preferred. Equation (5) is valid for the current modulation strategy A. Changing the input current modulation strategy leads to slightly different output power limits.

In [17] it has been shown that the power limit can be sensibly improved if the calculation of the duty-cycles is carried out by filtering the MC input voltages by means of a digital low-pass filter implemented in a synchronous reference frame.

The continuous-time equation representing such a filter applied to the input voltage vector is as follows

$$\frac{d\overline{v}_{if}}{dt} = \frac{\overline{v}_i - \left(1 - j\omega_i\tau\right)\overline{v}_{if}}{\tau} \tag{6}$$

where ω_i is the angular frequency of the input voltage source. By varying the time constant τ of the low-pass filter is possible to increase the limit voltage transfer ratio until the maximum value 0.866. The only drawback is that the filter may affect to some extent the capability of the control system to compensate the effect of input voltage disturbances on the load currents.

5 BIDIRECTIONAL SWITCHES

The MC requires bidirectional switches with the capability to block the voltage and to conduct the current in both directions. There are two main topologies for bidirectional switches, namely the

Fig. 5 Bidirectional switches: a) common emitter configuration, b) common collector configuration

common emitter anti-parallel IGBT configuration and the common collector anti-parallel IGBT configuration.

The common emitter arrangement is represented in Figure 5a. As known, two IGBTs are connected with two diodes in an anti-parallel configuration. The diodes provide the reverse blocking capability. The main advantage of this solution is that the two IGBTs can be driven with respect the same point, i.e. the same common emitter, that can be considered as a local ground for the bidirectional switch. On the other hand, each bidirectional switch requires an insulated power supply, in order to ensure a correct operation. Therefore, a total of nine insulated power supplies is needed.

The common collector arrangement is presented in Figure 5b. The IGBTs are now arranged in a common collector configuration. In this case, only six insulated power supplies are needed. In fact, three IGBTs have the emitter connected to the input phase a. This common point can be considered as a local ground for them. Furthermore, three other IGBTs have the emitter connected to the output phase A. Once again, this point has the meaning of a local ground, that has to be insulated from the previous one. The same can be repeated for the couples of phases b-B and c-C, thus concluding that six insulated power supplies are necessary. The complete connection scheme of the common collector arrangement is shown in Figure 6.

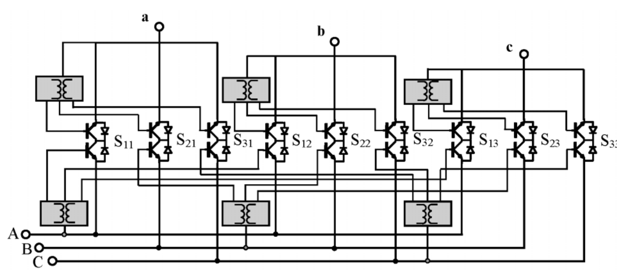

Fig. 6 Complete scheme of the power stage using common collector arrangement

For the MC described in this paper prototypes of new power modules, rated 50 A and 1200 V, have been adopted. Figure 7 shows one power module and Figure 8 shows the complete connection scheme.

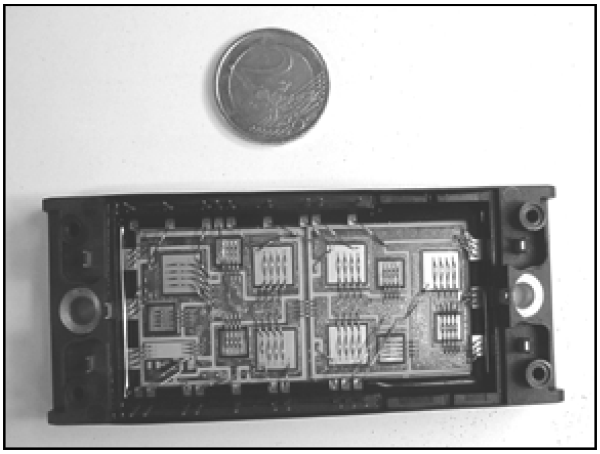

Fig. 7 View of the internal connection of the integrated power module

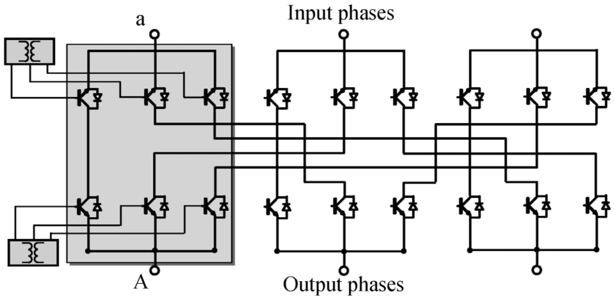

Fig. 8 Scheme of the power stage based on the new power modules

In this case each module contains three IGBTs connected to one input phase and three IGBTs connected to the corresponding output phase. The arrangement shown in Figure 8 is particularly suitable for the common collector configuration and allows a simplification of the control circuit layout, since each power module requires only two insulated supplies to be driven. The traditional solution, instead, requires four of the six insulated voltages that are necessary for the common collector configuration [19].

6 CURRENT COMMUTATION

Matrix converters have not free-wheeling diodes, like traditional voltage source inverters. This makes the current commutation between switches a difficult task, because the commutation has to be constantly controlled. The switches have to be turned on and off in such a way as to avoid short circuits and sudden current interruptions. Many commutation strategies have been already studied. The most common solution is the »4-step commutation«, that requires information about the actual current direction in the output phases. The four step sequence is shown in Figure 9, that refers to the general case of current commutation from a bidirectional switch »a« to a bidirectional switch »b«.

In the beginning both IGBT of switch »a« are enabled. In the first step, the IGBT S_{an}, which is not conducting the load current, is turned off. In the second step, the IGBT S_{bn}, that will conduct the current, is turned on. As a consequence, both switches »a« and »b« can conduct only positive currents and short circuits are prevented. Depending upon the instantaneous input voltages, after the second step, the conducting diode of switch »a« could be reverse biased and a natural commutation could take place. Otherwise, a hard commutation happens when, in the third step, IGBT S_{ap} is turned off. Finally, in the fourth step, the non-conducting switch S_{bn} is enabled to allow the conduction of negative currents too. During a period of the input voltage, the natural commutation occurs in 50 % of all commutations and therefore this current commutation has earned the name »semisoft switching«.

7 PRACTICAL IMPLEMENTATION

The MC prototype is shown in Figure 10. On the right there is the power board, mounted on the dissipation sink, in the middle the control unit and on the left the logic device devoted to the commutation control.

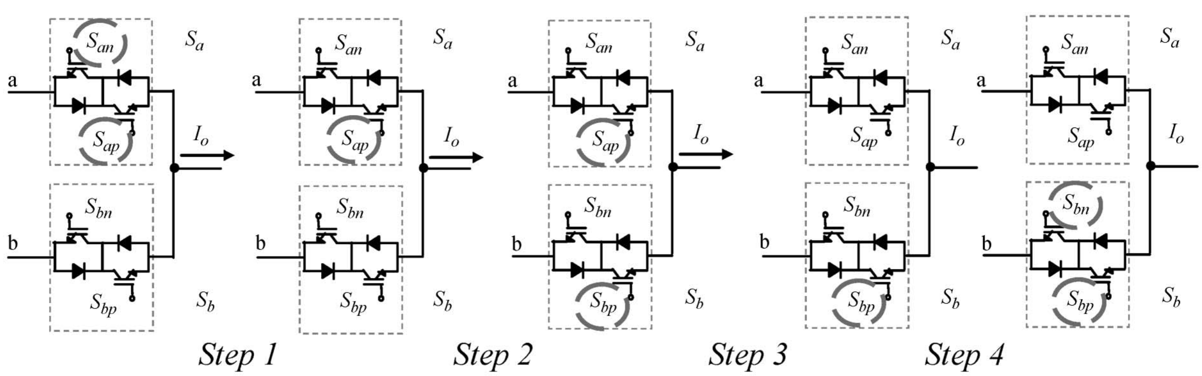

Fig. 9 Four step commutation sequence

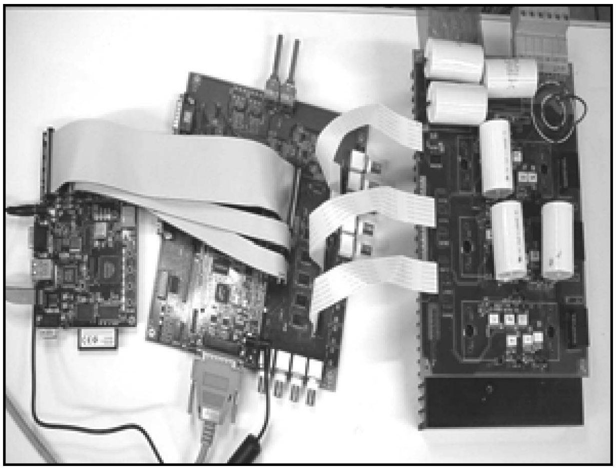

Fig. 10 View of the matrix converter set-up

A. Control unit

The calculation of the output voltage and input current reference as well as the calculation of the switch duty-cycle is performed by a single fixed--point digital signal processor (DSP). The adopted DSP is the TMS320F2812 by Texas Instruments, running at 150 MHz. The DSP is mounted on an evaluation board EzDSP manufactured by Spectrum Digital, which provides the basic interfaces for the use of the DSP.

The control of the commutation process, instead, is performed by a Cyclone EP1C20, a FPGA chip manufactured by Altera, running at 50 MHz. The commutation time is about 2 μs.

B. Space Vector Modulation

The MC prototype is controlled according to SVM principle. The modulation strategy adopted is »double-sided« or »symmetrical«, meaning that the turn-on sequence of the switches is completed in the first half of the cycle period and it is repeated with inverse order in the second half of the cycle period. The cycle period is 125 μs, corresponding to a switching frequency of 8 kHz.

C. Compensation of the commutation time

The 4-step commutation strategy requires a minimum time to be performed, that could be higher than the application time of an active configuration. This determines a deterioration of the input currents and of the output voltages, since the active configuration is not applied for a sufficient time.

For a given cycle period, the minimum commutation time determines a minimum value $\delta_{\min}$ for the duty-cycle of the active configurations and the zero configurations.

In order to improve the current quality, a simple compensation law has been implemented. Any duty--cycle lower than $\frac{1}{2}\delta_{\min}$ has been ignored, whereas any duty-cycle greater than $\frac{1}{2}\delta_{\min}$ and lower than $\delta_{\min}$ has been approximated to $\delta_{\min}$ min, as follows:

$$\delta_{\text{compensated}} = \begin{cases} 0 \text{ if } \delta < \frac{1}{2}\delta_{\min} \\ \delta_{\min} \text{ if } \frac{1}{2}\delta_{\min} < \delta < \delta_{\min} \end{cases} . \quad (7)$$

Although this compensation strategy is very simple to be implemented, it can greatly improve the current waveform, as it will be demonstrated in the Section regarding the experimental tests.

D. Converter protections

Due to the lack of free-wheeling paths for the currents, a number of protection strategies have been adopted to prevent the damage of the converter. Protections against over-load, short-circuit and over-voltage have been implemented.

The over-load protection is performed directly by the DSP, that turns off all the switches when the load current is greater than the rated one. This solution is not satisfactory in order to avoid the damage of the switches if a load short-circuit happens, because the latency time of the DSP depending on the cycle period is too high. Therefore, the protection against the short circuit consists in the monitoring of the collector-emitter voltage of all the IGBTs comprised in the power modules. This task is performed by eighteen components HCPL316, that are sufficient to drive the power modules.

It is worth noting that it is not possible to simply turn off all the switches, otherwise the inductive load current have no closing path. The most common solution to this problem is to add a diode bridge clamp across the input and the output sides of the converter, as shown in Figure 11. The small capacitor of the clamp is designed to store the energy corresponding to the inductive load current with an acceptable overvoltage.

In addition the voltage across the capacitor is continuously measured. In fact fault conditions are

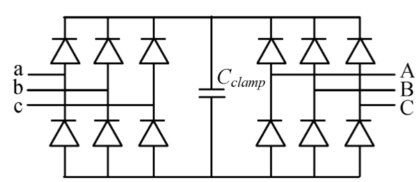

Fig. 11 Clamp circuit for the protection of the matrix converter

more frequently caused by instability phenomena at the input of the converter or wrong switch commutations rather than short circuits of the load. When the voltage across the capacitor becomes greater than a limit value, the over-voltage protection stops the converter.

8 EXPERIMENTAL RESULTS

Preliminary tests with a R-L passive load have been performed to verify the effectiveness of the solutions adopted.

Figure 12 shows the load current and the line-to-line load voltage for a voltage transfer ratio $q = 0.6$.

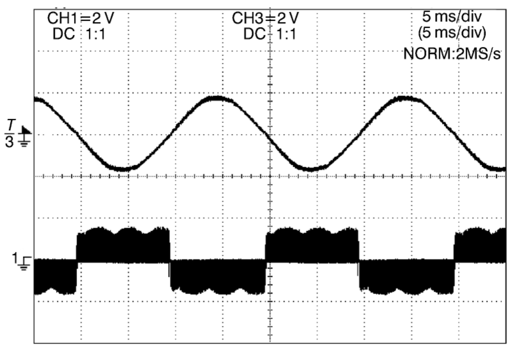

Fig. 12 Experimental test. Behaviour of MC in steady-state conditions. Upper trace: load current (10 A/div). Lower trace: line to line output voltage (400 V/div)

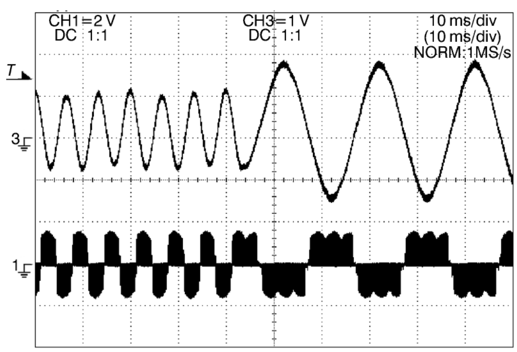

Fig. 13 Experimental test. Behaviour of MC during a output frequency step. Upper trace: load current (5 A/div). Lover trace: line to line output voltage (400 V/div)

In order to test the behavior of the converter after a sudden load variation, the reference voltage has been changed from $q = 0.3$ to $q = 0.6$ and the output frequency has been decreased from 100 Hz to 50 Hz. Figure 13 shows the load current and the line-to-line load voltage during the transient. As can be seen, the output current remains nearly sinusoidal.

To verify the effectiveness of the compensation strategy given by (7), three different tests have been carried out at low load current. Figure 14 reports the load current and the load line-to-line voltages corresponding to the three tests. In the first test (Figure 14a), any duty cycle lower than $\delta_{\min}$ was replaced by $\delta_{\min}$. In the second test (Figure 14b), any duty-cycle lower than $\delta_{\min}$ was ignored. Finally, in the third test (Figure 14c), the compensation law (7) was adopted. It can be noted that, although this law is extremely simple, it significantly improves the quality of the load current.

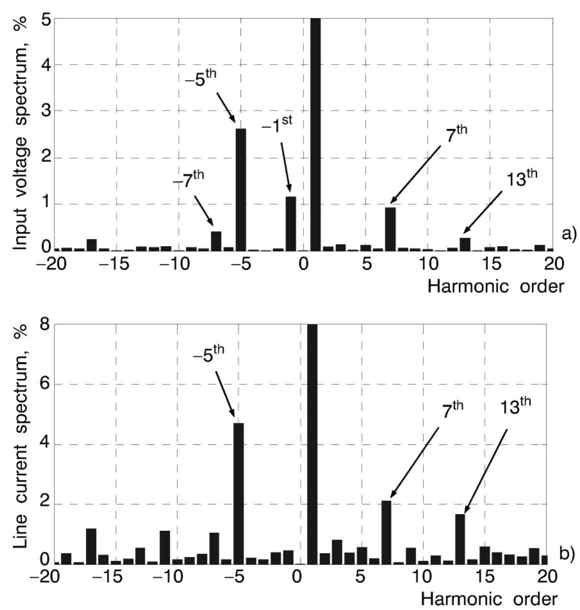

Fig. 15 Experimental result. MC behaviour with distorted input voltage. a) Spectrum of the input voltage vector, in percent of the fundamental component. b) Spectrum of the line current vector, in percent of the fundamental component

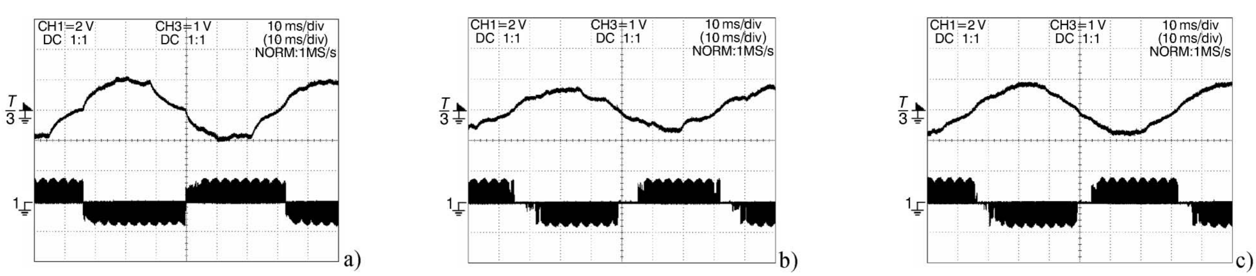

Fig. 14 Experimental tests. Behaviour of MC with and without compensation of the commutation times. Upper trace: load current. Lower trace: line to line output voltage. a) duty-cycles < δ_{min} are set to δ_{min}, b) duty-cycles < δ_{min} are ignored, c) with compensation

Finally, a test was carried out in condition of distorted input voltage. The spectra of the input voltage and the line currents are shown in Figure 15. As can be seen, the absence of reactive elements does not let the MC to generate sinusoidal line currents. The line currents contains almost the same harmonics of the input voltage.

9 CONCLUSIONS

This paper presents the implementation of a digitally controlled MC based on a fixed-point DSP TMS320F28 and new prototype of power modules.

This paper is mainly focused on the technical solutions adopted to obtain good performances of the converter. Several experimental results are provided to show the effectiveness of the adopted solutions.

REFERENCES

[1] A. Alesina, M. Venturini, **Solid-State Power Conversion: a Fourier Analysis Approach to Generalized Transformer Synthesis.** IEEE Trans. Circuits and Systems, vol. 28, No. 4, pp. 319–330, April 1981.

[2] A. Alesina, M. G. B. Venturini, **Analysis and Design of Optimum-Amplitude Nine-Switch Direct AC-AC Converters.** IEEE Trans. Power Electronics, vol. 4, pp. 101–112, January 1989.

[3] P. D. Ziogas, S. I. Khan, M. H. Rashid, **Analysis and Design of Forced Commutated Cycloconverter Structures with Improved Transfer Characteristics.** IEEE Trans. Industrial Electronics, vol. 1E-33, No. 3, pp. 271–280, August 1986.

[4] L. Huber, D. Borojevic, **Space Vector Modulator for Forced Commutated Cycloconverters.** In Proc. IEEE PESC Conf., San Diego, (USA), 1989, pp. 871–876.

[5] L. Huber, D. Borojevic, **Space Vector Modulated Three--Phase to Three-Phase Matrix Converter with Input Power Factor Correction.** IEEE Trans. on IA, Vol. 31, No. 6, November/December 1995, pp. 1234–1246.

[6] D. Casadei, G. Grandi, G. Serra, A. Tani, **Space Vector Control of Matrix Converters with Unity Input Power Factor and Sinusoidal Input/output Waveforms.** In Proc. EPE Conference, Brighton (UK), 13–16 September 1993, vol. 7, pp. 170–175.

[7] L. Helle, K. B. Larsen, A. H. Jorgensen, S. Munk-Nielsen, **Evaluation of Modulation Schemes for Three-Phase to Three-Phase Matrix Converters.** IEEE Trans. Industrial Electroncs, Vol. 51, No. 1, pp. 158–171, February 2004.

[8] D. Casadei, G. Serra, A. Tani, L. Zarri, **Matrix Converter Modulation Strategies: A New General Approach Based on Space-Vector Representation of the Switch State.** IEEE Trans. Industrial Electronics, Vol. 49, No. 2, pp. 370–381, April 2002.

[9] C. Klumpner, P. Nielsen, I. Boldea, F. Blaabjerg, **New Solutions for a Low-cost Power Electronic Building Block for Matrix Converters.** IEEE Trans. on Industrial Electronics, Vol. 49, No. 2, Apr. 2002, pp. 336–344.

[10] J. Mahlein, J. Weigold, O. Simon, **New Concepts for Matrix Converter Design.** IEEE IECON'01, 29 Nov.–2 Dec. 2001, Denver, USA, vol. 2, pp.1044–1048.

[11] M. Bland, L. Empringham, P. W. Wheeler, J. C. Clare, **Comparison of Calculated and Measured Switching Lasses in Direct AC-AC Converters.** IEEE PESC Conf 2001, pp. 1096–1101.

[12] Jun-Koo Kang, H. Hara, E. Yamamoto, E. Watanabe, **Analysis and Evaluation of Bi-directional Power Switch Losses for Matrix Converter Drive.** Record of the Industry Applications Conference 2002, 13–18 Oct. 2002, pp. 438–443, vol. 1.

[13] K. G. Kerris, P. W. Wheeler, J. C. Clare, L. Empringham, **Implementation of a Matrix Converter Using p-channel MOS-controlled Thyristors, Power Electronics and Variable Speed Drives.** 2000. Eighth International Conference on IEE Conf. Publ. No. 475, 18–19 Sept. 2000, pp. 35–39.

[14] P. W. Wheeler, J. C. Clare, L. Empringharn, M. Bland, M. Apap, **Gate Drive Level Intelligence and Current Sensing for Matrix Converter Current Commutation.** IEEE Trans. on Industrial Electronics, Vol. 49, No. 2, April 2002, pp. 382–389.

[15] D. Casadei, A. Trentin, M. Matteini, M. Calvini, **Matrix Converter Commutation Strategy Using Both Output Current and Input Voltage Sign Measurement.** EPE 2003, 2–4 Sept., Toulouse, France, paper 1101, CD-ROM.

[16] P. Wheeler, D. Grant, **Optimised Input Filter Design and Low-loss Switching Techniques for a Practical Matrix Converter.** IEE Proc. Electric Power Applications, Vol. 144, Issue: 1, Jan. 1997, pp. 53–60.

[17] D. Casadei, G. Serra, A. Tani, L. Zarri, **Effects of Input Voltage Measurement on Stability of Matrix Converter Drive System.** IEE Proceedings on Electric Power Applications, vol. 151, No. 4, July 2004, pp. 487–497.

[18] T. F. Podlesak, D. Katsis, P. W. Wheeler, J. C. Clare, L. Empringham, M. Bland, **A 150 kVA Vector Controlled Matrix Converter Induction Motor Drive.** Record of the IEEE Industry Applications Conference, 2004, 3–7 Oct. 2004, vol. 3, pp. 1811–1816.

[19] Yanhui Xie, Yongde Ren, **Implementation of DSP-based Three-phase AC-AC Matrix Converter.** Proc. of IEEE APEC '04, vol. 2, 2004, pp. 843–847.

[20] P. W. Wheeler, J. C. Clare, L. Empringham, **A Vector Controlled MCT Matrix Converter Induction Motor Drive with Minimized Commutation Times and Enhanced Waveform Quality.** Prof. of IEEE IAS 2002, Vol. 1, 13–18 Oct. 2002, pp. 466–472.

[21] D. Casadei, G. Serra, A. Tani, **A General Approach for the Analysis of the Input Power Quality in Matrix Converters.** IEEE Trans. on PE, vol. 13, n. 5, September 1998, pp. 882–891.

[22] F. Blaabjerg, D. Casadei, C. Klumpner, M. Matteini, **Comparison of Two Current Modulation Strategies for Matrix Converters under Unbalanced Input Voltage Conditions.** IEEE Trans. on IE, vol. 49, n. 2, April 2002, pp. 289–296.

[23] D. Casadei, G. Serra, A. Tani, L. Zarri, **Stability Analysis of Electrical Drives Fed by Matrix Converters.** In Proceedings of IEEE-ISIE 2002, L'Aquila, Italy, July 8-11, 2002.

Eksperimentalno ponašanje prototipa matričnog pretvarača izvedenog s novim energetskim modulima. Članak opisuje projekt i rješenja usvojena za prototip 10 kW matričnog pretvarača, izvedenog s novim integriranim energetskim modulima. Svojstva pretvarača provjerena su eksperimentalnim ispitivanjima.

Ključne riječi: matrični pretvarač, elektromotorni sustav s pretvaračem, modulacijska strategija, strategija za komutaciju struje, integrirani elektronički energetski modul

AUTHORS' ADDRESSES

Domenico Casadei
Giovanni Serra
Angelo Tani
Luca Zarri

Dept. of Electrical Engineering, Bologna, Italy

Received: 2005-12-01